

Spray Stress Revisited

EDGAR L ANDREAS

U.S. Army Cold Regions Research and Engineering Laboratory, Hanover, New Hampshire

(Manuscript received 24 April 2003, in final form 12 January 2004)

ABSTRACT

In winds approaching hurricane strength, spray droplets proliferate. Once created, these droplets accelerate to the local wind speed in 1 s or less and thereby extract momentum from the wind. Because these droplets have substantial mass, they eventually plunge back into the ocean, delivering their horizontal momentum to the surface in the form of a spray stress. Inadequate information on the production rate and size distribution of spray droplets, however, hampered previous attempts to estimate the magnitude of this spray-mediated momentum exchange. This paper therefore uses recent estimates of the spray generation function to reconsider spray's ability to alter air–sea momentum exchange. Conservation of momentum requires that spray cannot enhance the air–sea stress beyond what the large-scale flow dictates. However, spray can redistribute stress in the near-surface atmosphere since the wind must slow if the spray droplets accelerate. For a wind of 30 m s^{-1} , spray supports about 10% of the surface stress; for a wind of about 60 m s^{-1} , spray supports all of the surface stress. The paper goes on to show how this partitioning affects the near-surface wind speed profile. Last, the paper reviews evidence that suggests the sea surface undergoes a transition in its aerodynamic behavior in the wind speed range $30\text{--}40 \text{ m s}^{-1}$. The fact that whitecap coverage extrapolates to 100% in this range may be one cause. Also in this range, the “rain” of spray droplets back onto the sea surface creates a mass flux with a magnitude that has been shown to damp the short waves that sustain most of the atmospheric drag on the sea surface. As a consequence, spray may play a key role in a negative feedback loop that limits air–sea momentum transfer.

1. Introduction

When sea spray droplets are thrown into the air, they accelerate almost immediately to the local wind speed. This process extracts momentum from the near-surface wind and therefore slows it. When these droplets then crash back into the sea, they transfer this momentum to the sea surface as a surface stress. Thus, conceptually at least, sea spray has the potential to alter the near-surface distributions of momentum and stress on both the air and water sides of the air–sea interface. Munk (1955) may have been the first to identify this process.

Others who have looked at spray's role in air–sea momentum exchange, however, generally found it insignificant. I will use the term *interfacial* stress to identify the usual air–sea momentum flux or surface stress, which we commonly parameterize with the 10-m wind speed (U_{10}), the air density (ρ_a), and the 10-m drag coefficient (C_{D10}) as

$$\tau_a = \rho_a C_{D10} U_{10}^2. \quad (1.1)$$

Considering only jet droplets, Monahan (1966) estimates that the spray stress in a near-surface wind of

9.1 m s^{-1} is less than 0.01 N m^{-2} —less than 10% of the interfacial stress at this wind speed. Wu (1973) concludes that, for wind speeds up to 14 m s^{-1} , the spray stress is less than 0.1% of the interfacial stress.

Fairall et al. (1994) do an analysis similar to Wu's (1973) but with better information about the behavior of the sea spray generation function. Remember, the spray generation function quantifies the rate at which spray droplets are produced at the sea surface as a function of droplet radius and wind speed (e.g., Andreas 2002). Fairall et al. conclude that the spray stress is about 10% of the interfacial stress when $U_{10} = 50 \text{ m s}^{-1}$ and is about 1% when $U_{10} = 20 \text{ m s}^{-1}$ (cf. Mestayer et al. 1996).

Pielke and Lee (1991) use a kinetic energy argument that is fundamentally different from these analyses by Wu (1973) and Fairall et al. (1994) to estimate how spray might alter the near-surface wind speed profile. Without referring to any of the papers on the near-surface distribution of spray that were available to them, they guess what the near-surface water loading from sea spray might be to complete their analysis. With a spray water loading right at the surface of 0.50 kg m^{-3} , their largest value, Pielke and Lee estimate that the wind speed at a height of 1 m would be retarded by about 2 m s^{-1} for 10-m wind speeds between 20 and 35 m s^{-1} . Although they do not also calculate how spray might

Corresponding author address: Dr. Edgar L. Andreas, U.S. Army Cold Regions Research and Engineering Laboratory, 72 Lyme Road, Hanover, NH 03755-1290.
E-mail: eandreas@crrel.usace.army.mil

affect the surface stress under such conditions, I estimate that, because of the decreased gradient in the wind speed profile right at the surface, the spray stress would constitute about 40% of the undisturbed interfacial stress for the conditions they model.

In reviewing Pielke and Lee's (1991) analysis, however, Fairall et al. (1994) conclude that the maximum spray water loading they assume is about 40 times too large, even if the wind speed were 40 m s^{-1} . Even the minimum water loading they consider, 0.05 kg m^{-3} , is 4 times too large. I concur with Fairall et al. that Pielke and Lee's analysis does not represent a realistic spray environment.

Caldwell and Elliott's (1971, 1972) studies of how rain might affect the surface stress and the near-surface wind speed profile are also pertinent here. In particular, they estimate the ratio of rain stress (τ_R) to the interfacial stress to be

$$\tau_R/\tau_a = 0.16R/U_{10}, \quad (1.2)$$

where R is the rainfall rate in millimeters per hour. They thus conclude that a high rainfall rate of several tens of millimeters per hour would make this ratio 20%–30% for wind speeds of $10\text{--}20 \text{ m s}^{-1}$.

Caldwell and Elliott's (1971, 1972) rain studies highlight some interesting differences with spray processes. The rain-at-sea problem, as posed by Caldwell and Elliott, is an open system. The raindrops form high in the atmosphere, fall through layers with relatively high wind speeds, and thus reach the near-surface atmospheric layer with relatively high horizontal speed. They thus decelerate in the slower flow within a few tens of meters above the sea surface and therefore transfer momentum to the near-surface flow. Because raindrops enter the system with relatively high horizontal speed, (1.2) shows that their relative effect on surface stress actually decreases as the 10-m wind speed increases—mainly because τ_a goes as U_{10}^2 [see (1.1)], while τ_R goes only as U_{10} .

The spray problem, in contrast, presents a closed system. The ocean creates spray droplets, they are airborne in the near-surface atmosphere for a while, and then they return to the ocean. Intuitively, we realize that spray may be able to redistribute momentum in the air and the sea, but its ability to change the total downward momentum flux is not obvious. Second, unlike the rain problem, the amount of airborne spray depends on the local wind speed—approximately as its third power (e.g., Andreas 2002). Spray effects may thus increase dramatically with increasing wind speed. In fact, Andreas and Emanuel (2001) infer that the spray stress goes as the fourth power of the friction velocity, u_{*} .

Here, I provide some of the details that are missing in Andreas and Emanuel's (2001) analysis and clear up some misconceptions in their work. In particular, Andreas and Emanuel assume that the spray stress just adds to the stress that would be present under similar conditions in the absence of spray. Because the spray system

is closed, however, this assumption violates conservation of momentum. As a result, I must revise some of Andreas and Emanuel's inferences.

With these new insights, I explain that spray's main role is to redistribute the wind's momentum in the near-surface layer. In other words, spray can slow the near-surface wind speed—by as much as 3 m s^{-1} in a 36 m s^{-1} wind. As a result, although the total surface stress may be the same as in the absence of spray, the spray contribution to that stress increases with wind speed while the interfacial contribution decreases.

Last, I suggest how spray might indirectly affect air–sea momentum coupling. Since the mass flux of the spray produced increases as the cube of u_{*} , and because most of this mass falls back onto the ocean surface, spray could suppress wave growth. That is, the spray may provide a regulating mechanism with negative feedback that limits air–sea momentum transfer. Simply put, higher winds build waves and produce more spray; but, in turn, more spray falls back on the surface and knocks down the waves.

2. Formulation for the spray stress

a. Mathematical background

Estimating how spray drags on the near-surface wind and transfers momentum to the sea surface is conceptually easy. The spray generation function dF/dr_0 quantifies how many spray droplets with initial radius r_0 are produced per square meter of surface per second per micrometer increment in droplet radius as a function of the 10-m wind speed U_{10} . If the spray droplets accelerate to horizontal speed $u_{sp}(r_0)$ before falling back into the sea, the rate at which they extract momentum from the air is (cf. Fairall et al. 1994; Andreas and Emanuel 2001)

$$\tau_{sp,air} = \frac{4\pi}{3}\rho_w \int_{r_{lo}}^{r_{hi}} \mu_{sp}(r_0)r_0^3 \frac{dF}{dr_0} dr_0. \quad (2.1)$$

Here, ρ_w is the density of seawater, and r_{lo} and r_{hi} are the lower and upper radius limits of the droplets that are important in this process. Typically, $r_{lo} \approx 1 \mu\text{m}$, and $r_{hi} \approx 500 \mu\text{m}$.

Likewise, we can formally express the spray stress on the sea surface by first defining the mass flux of droplets with radius r falling back on the sea. This is

$$M_{sp}(r) = \frac{4\pi}{3}\rho_w r^3 u_f(r) C_0(r), \quad (2.2)$$

where $u_f(r)$ is the terminal fall speed of droplets with radius r (e.g., Andreas 1990), and $C_0(r)$ is the near-surface number concentration of these droplets.

If droplets with radius r hit the sea surface with a horizontal speed of $u_{sp}(r)$, the total sea surface stress they impart is thus

$$\tau_{sp,ss} = \frac{4\pi}{3}\rho_w \int_{r_{lo}}^{r_{hi}} u_{sp}(r)u_f(r)r^3 C_0(r) dr. \quad (2.3)$$

I formulate (2.2) and (2.3) in terms of r rather than r_0 to acknowledge that the spray droplets may lose some mass by evaporation during their brief flights above the sea surface.

But a common assumption in this field is that, at least for the droplet sizes relevant to spray momentum transfer, the near-surface spray distribution is in equilibrium (e.g., Moore and Mason 1954; Fairall and Larsen 1984; Andreas and DeCosmo 1999). That is, the rate at which droplet mass is produced is equal to the rate at which droplet mass falls back into the sea. Mathematically, this equilibrium requires

$$r_0^3 \frac{dF}{dr_0} = u_f(r)r^3 C_0(r). \quad (2.4)$$

In the very high winds that are my focus here, the near-surface relative humidity will be well above 90%. Consequently, the massive droplets that contribute most to the integrals in (2.1) and (2.3) will shrink by evaporation by, at most, 20% in radius (or by less than 50% in mass) (Andreas 1990). Thus, from (2.4),

$$\frac{dF}{dr_0} \approx u_f(r_0)C_0(r_0). \quad (2.5)$$

As a result, the rate at which spray extracts momentum from the air, $\tau_{sp,air}$ in (2.1), is nearly equivalent to the stress that spray imparts to the sea surface, $\tau_{sp,ss}$ in (2.3):

$$\tau_{sp} \equiv \tau_{sp,air} \geq \tau_{sp,ss}. \quad (2.6)$$

Henceforth, by *spray stress*, τ_{sp} , I can mean either (2.1) or (2.3), although I will use (2.1) to compute the greatest upper bound on the spray stress. And this estimate will be no more than a factor of 2 greater than $\tau_{sp,ss}$.

Evaluating (2.1) requires only two pieces of information: the spray generation function dF/dr_0 and the horizontal speed $u_{sp}(r_0)$ that spray droplets reach before falling back into the sea. Andreas (2002) collects and reviews the spray generation functions available in the literature and identifies several reliable candidates for this function. Therefore, I next evaluate the droplet speed $u_{sp}(r_0)$.

b. Horizontal droplet speed

The horizontal force balance on an airborne spray droplet of radius r_0 in a mean wind of speed U is (e.g., Wu 1979b; Raupach 1991)

$$\frac{1}{2} \pi r_0^2 \rho_a C_d(\text{Re})(U - u_d)^2 = \frac{4\pi}{3} r_0^3 \rho_w \frac{du_d}{dt}. \quad (2.7)$$

Here, ρ_a and ρ_w are again the air and water densities, u_d is the instantaneous horizontal speed of the droplet, and $C_d(\text{Re})$ is the drag coefficient of a spherical droplet with Reynolds number

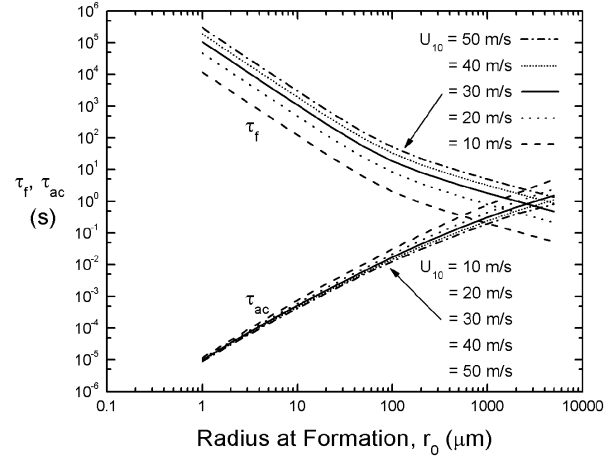


FIG. 1. The time τ_{ac} required for sea spray droplets starting with no horizontal speed to accelerate to within e^{-1} of the indicated wind speed U_{10} . Here, τ_f is the typical atmospheric residence time for droplets of initial radius r_0 at the indicated wind speed [see (2.10)]. For these calculations, the air temperature is 20°C, and the barometric pressure is 1000 hPa.

$$\text{Re} = \frac{(U - u_d)(2r_0)}{\nu}, \quad (2.8)$$

where ν is the kinematic viscosity of air.

On rearranging (2.7), I get

$$\frac{du_d}{dt} = \frac{3}{8} C_d(\text{Re}) \frac{\rho_a}{\rho_w} \frac{(U - u_d)^2}{r_0}. \quad (2.9)$$

I solved this for u_d as a function of time with a fourth-order Runge–Kutta formula (Press et al. 1992, 701–708). For $C_d(\text{Re})$ here, I used the relations for various Re ranges given in Table 5.2 of Clift et al. (1978, p. 112).

I integrated (2.9) until u_d was within 1% of U . Along the way, I also identified the time τ_{ac} , from creation of the droplet, for which u_d was within e^{-1} of U . That is, at τ_{ac} , the droplet has accelerated from rest to speed $(1 - e^{-1})U = 0.632U$. Figure 1 shows τ_{ac} for droplets with radii at formation between 1 and 5000 μm . This time to accelerate is a function also of the local wind speed since the droplet drag coefficient depends on this through the Reynolds number (2.8). As a reference standard, I use the 10-m wind speed for U in (2.7)–(2.9) and in Fig. 1.

Figure 1 shows that droplets for which $r_0 \leq 500 \mu\text{m}$, where we have reliable values for the spray generation function, reach 63% of the local wind speed in much less than a second. Notice that droplets take longer to reach this limit in 10 m s⁻¹ winds than in 50 m s⁻¹ winds because the initial drag force on a droplet is approximately 25 times as great at 50 m s⁻¹. Nevertheless, the difference in acceleration times for the different wind speeds is less than an order of magnitude for all droplets in Fig. 1.

To decide whether the τ_{ac} values depicted in Fig. 1

limit the momentum exchange that the spray can mediate, we need an estimate of how long the droplets remain airborne. For an estimate of this residence time, Andreas (1992) introduces

$$\tau_f = \frac{A_{1/3}}{u_f(r_0)}, \quad (2.10)$$

where $u_f(r_0)$ is again the fall velocity of a droplet with radius r_0 , and $A_{1/3}$ is the significant wave amplitude, which I estimate as (Andreas 1992)

$$A_{1/3} = 0.015U_{10}^2. \quad (2.11)$$

Here, $A_{1/3}$ is in meters when U_{10} is in meters per second. The largest droplets that carry most of the spray momentum form as spume at the crests of waves. Equation (2.10) therefore simply estimates how long these droplets take to fall back into the sea. Figure 1 also shows τ_f as a function of r_0 and U_{10} .

According to Fig. 1, except for wind speeds of 10 m s^{-1} and less, all droplets up to $500 \mu\text{m}$ in radius are airborne for at least 1 s. Because the wave amplitude grows with wind speed, higher wind speeds allow the droplets even longer to accelerate to the local wind speed.

On comparing τ_{ac} and τ_f in Fig. 1, I conclude that, for the wind speeds I treat here, all droplets with radii up to $500 \mu\text{m}$ will be essentially traveling at the local wind speed. Schmidt's (1982) measurements of particle speed and wind speed in blowing snow corroborate this conclusion. Therefore, in (2.1), $u_{sp}(r_0)$ is independent of r_0 ; I estimate it from

$$U(z) = \frac{u_*}{k} \ln\left(\frac{z}{z_0}\right), \quad (2.12)$$

where $U(z)$ is the wind speed at height z , and k ($=0.40$) is the von Kármán constant. In writing (2.12), I also implicitly assume that stratification effects on the wind speed profile are negligible for the high wind speeds that are my focus. To estimate u_{sp} , I substitute $A_{1/3}$ for z in (2.12).

In (2.12), I model the roughness length z_0 with Charnock's relation,

$$z_0 = 0.0185 \frac{u_*^2}{g}, \quad (2.13)$$

where g is the acceleration of gravity. The value I use for the Charnock constant in (2.13), 0.0185, is a typical value for the young waves that likely exist in high winds (e.g., Wu 1982b; Johnson et al. 1998; Toba et al. 2001; Andreas and Emanuel 2001). In (2.13), z_0 is in meters when u_* and g are in MKS units.

c. Spray stress

Figure 2 shows estimates of the spray stress computed from (2.1) for droplets with radii from 1–2 to $500 \mu\text{m}$. For dF/dr_0 in (2.1), I use three spray generation func-

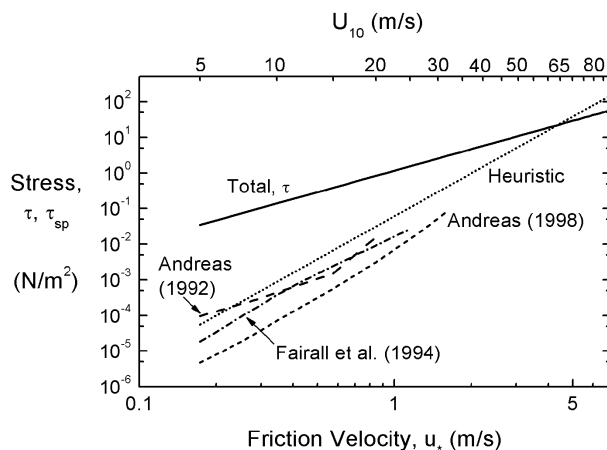


FIG. 2. Estimates of the spray stress computed from (2.1) for the spray generation functions from Andreas (1992, 1998) and Fairall et al. (1994). The extent of these curves reflects the wind speed range over which the functions are appropriate. The “Heuristic” line comes from Andreas and Emanuel (2001) and is (2.14). For comparison, the total stress is just $\tau = \rho_a u_*^2$.

tions that Andreas (2002) concludes are reliable for droplets in this size range and for the various wind speed limits shown in the figure. The figure also shows the total stress imposed by the large-scale flow, which I take as $\tau = \rho_a u_*^2$. This flow therefore also sets u_* .

Figure 2 corroborates the analyses by Wu (1973) and Fairall et al. (1994): For wind speeds of 30 m s^{-1} and less, where we have observations, the spray stress is, at most, 10% of the total (mostly interfacial) stress. The total stress, however, goes as the square of u_* , while Fig. 2 suggests that the spray stress depends more strongly on u_* . Andreas and Emanuel (2001) first suggested that τ_{sp} goes as the fourth power of u_* . This behavior is fairly easy to see: In (2.1), dF/dr_0 goes approximately as u_*^3 (e.g., Andreas 2002), while from (2.12), $u_{sp}(r_0)$ goes as u_* . The calculations of τ_{sp} in Fig. 2 that are based on the spray generation functions of Andreas (1992, 1998) and Fairall et al. (1994) all tend to approximate this u_*^4 dependence.

Andreas and Emanuel (2001) therefore assume that τ_{sp} is proportional to u_*^4 and tune the proportionality constant to agree with calculations in Fig. 2 and to produce reasonable simulations in Emanuel's (1995) tropical cyclone model. Their result is the “Heuristic” line in Fig. 2,

$$\tau_{sp} = 6.2 \times 10^{-5} \rho_w u_*^4, \quad (2.14)$$

which gives τ_{sp} in newtons per meter squared when ρ_w is in kilograms per meter cubed and u_* is in meters per second. I henceforth take (2.14) as a simple estimate of the spray stress.

Notice in Fig. 2 how (2.14) behaves. Since it goes as u_*^4 , it eventually becomes comparable to the total stress for 10-m wind speeds above 50 m s^{-1} . Of course, we have no irrefutable evidence that τ continues increasing with wind speed as suggested in Fig. 2 for wind speeds

above 30–40 m s⁻¹. Stress τ must go as u_*^2 by definition. However, the relation between U_{10} and u_* in Fig. 2 (and in later figures) is through (2.12) with z_0 given by (2.13), which I have extrapolated far beyond the wind speed range for which it has been verified.

Likewise, the increase in spray stress that (2.14) predicts is also very speculative. My justification for making these predictions, though, is that our understanding of the physics for lower wind speeds suggests them, and we need such theoretical guidelines to improve predictions for the intensity of ocean storms (e.g., Emanuel 1999; Lighthill 1999; Andreas and Emanuel 2001).

3. Effect on the wind speed profile

Caldwell and Elliott (1971, 1972) and Pielke and Lee (1991) estimate how water droplets influence the near-surface wind speed profile. Caldwell and Elliott study the force balance on raindrops to make their estimates. Pielke and Lee assume that the kinetic energy at height z is conserved for the wind and droplet system and then assume a profile of suspended water mass to estimate how spray affects the wind speed profile.

Here though, I take a third approach that comes from the literature on saltation—for example, Radok (1968), Pomeroy and Male (1987), and Raupach (1991). This is basically a conservation of momentum argument in which I assume that the total stress is constant with height in an atmospheric surface layer. As above, I denote this total stress as $\tau = \rho_a u_*^2$; in a large-scale model, it might come from a geostrophic drag relation or, as in Andreas and Emanuel’s (2001) hurricane model, from a gradient wind relation. Belcher and Hunt (1993), Kudryavtsev and Makin (2001), and Hara and Belcher (2002), among others, similarly assume that τ is constant with height in the wave boundary layer, where they partition that total stress among several components.

In the droplet evaporation layer, I partition τ between the stress supported by the air, $\tau_a(z)$, and by the sea spray, $\tau_{sp}(z)$ (cf. Pomeroy and Male 1987; Raupach 1991). That is,

$$\tau \equiv \rho_a u_*^2 = \tau_a(z) + \tau_{sp}(z). \quad (3.1)$$

In analogy with τ and u_* , I can define a local friction velocity $u_*(z)$ from the local air stress such that

$$\tau_a(z) = \rho_a [u_*(z)]^2. \quad (3.2)$$

Equations (3.1) and (3.2) provide an estimate of $u_*(z)$ from quantities we know:

$$u_*(z) = \left[u_*^2 - \frac{\tau_{sp}(z)}{\rho_a} \right]^{1/2}. \quad (3.3)$$

However, I can also estimate $\tau_a(z)$ from first-order closure, as usual in an atmospheric surface layer;

$$\tau_a(z) = \rho_a K_m(z) \frac{dU}{dz}, \quad (3.4)$$

where dU/dz is the vertical gradient in wind speed. Even in a flow with suspended particles, it is common to model the turbulent diffusivity for neutral stratification as (e.g., Fairall et al. 1990; Rouault et al. 1991; Wamser and Lykossov 1995; Bintanja 1998; Xiao and Taylor 2002)

$$K_m(z) = k u_*(z) z, \quad (3.5)$$

which, with (3.3), becomes

$$K_m(z) = kz \left[u_*^2 - \frac{\tau_{sp}(z)}{\rho_a} \right]^{1/2}. \quad (3.6)$$

Although in high winds the droplets most relevant to momentum transfer are created as spume droplets near the wave crests, these diffuse both up and down to produce relatively smooth droplet profiles (e.g., de Leeuw 1986, 1987). From modeling results (i.e., Andreas et al. 1995; Edson et al. 1996; Mestayer et al. 1996), Andreas and DeCosmo (1999) develop a speculative profile for the concentration C of droplets with radius r_0 at height z ,

$$C(z, r_0) = C_0(r_0) \exp\left(\frac{z \ln b}{2A_{1/3}}\right). \quad (3.7)$$

Here, $C_0(r_0)$ is again the surface concentration of droplets with radius r_0 , b is a constant taken as 0.001, and $A_{1/3}$ comes from (2.11).

Other expressions for $C(z, r_0)$ exist; Toba’s (1965) may be the best-known alternative. Fairall et al. (1990) update Toba’s formulation, and their result has several similarities with (3.7). Namely, both predict $C(z, r_0)$ as exponential functions of z , scale z with a length scale connected to the height where the droplets originate, and scale $C(z, r_0)$ with the concentration of droplets with radius r_0 at a fixed height. I prefer (3.7) because it is computationally simpler and I have had more experience using it.

Since spray droplets accelerate to the local wind speed almost immediately, as a first approximation, I can assume that the spray stress profile, $\tau_{sp}(z)$ in (3.1), also has a form like (3.7). Since I have already established that (2.14) gives the spray stress right at the surface $\tau_{sp}(0)$, I simply write by analogy with (3.7) that

$$\tau_{sp}(z) = \tau_{sp}(0) \exp\left(\frac{z \ln b}{2A_{1/3}}\right). \quad (3.8)$$

On substituting (3.4), (3.6), and (3.8) into (3.1), I get a differential equation for the wind speed profile when spray is present,

$$\begin{aligned} \rho_a u_*^2 = & \rho_a kz \left[u_*^2 - \frac{\tau_{sp}(0)}{\rho_a} \exp\left(\frac{z \ln b}{2A_{1/3}}\right) \right]^{1/2} \frac{dU}{dz} \\ & + \tau_{sp}(0) \exp\left(\frac{z \ln b}{2A_{1/3}}\right), \end{aligned} \quad (3.9)$$

or, with some rearranging,

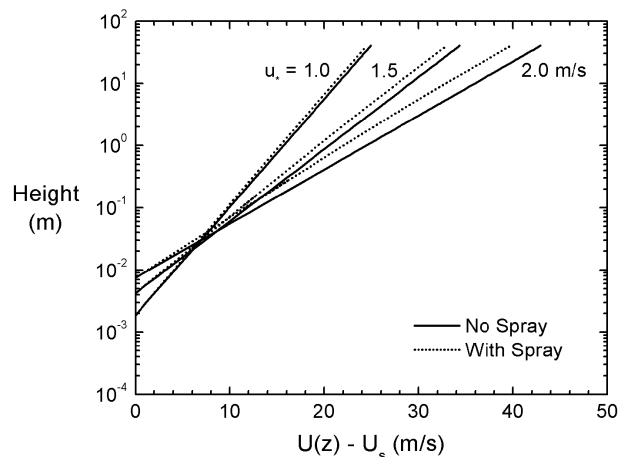


FIG. 3. Near-surface wind speed profiles with and without spray present as a function of the friction velocity u_* . These results come from integrating (3.11). For these calculations, the air temperature is 20°C, and the barometric pressure is 1000 hPa.

$$\frac{dU}{dz} = \frac{u_* - \frac{\tau_{sp}(0)}{\rho_a k z u_*} \exp\left(\frac{z \ln b}{2A_{1/3}}\right)}{\left[1 - \frac{\tau_{sp}(0)}{\rho_a u_*^2} \exp\left(\frac{z \ln b}{2A_{1/3}}\right)\right]^{1/2}} \quad (3.10)$$

The $\tau_{sp}(0)$ term in the denominator here is much smaller than 1. Hence, (3.10) essentially reduces to

$$\frac{dU}{dz} = \frac{u_*}{kz} - \frac{6.2 \times 10^{-5} \rho_w u_*^3}{2\rho_a kz} \exp\left(\frac{z \ln b}{2A_{1/3}}\right), \quad (3.11)$$

where I keep terms only to first order in $\tau_{sp}(0)$ and have used (2.14) to replace $\tau_{sp}(0)$.

We see from (3.11) that $U(z)$ approaches the usual semilogarithmic profile for large z . However, near the surface, the spray reduces the wind speed gradient and retards the wind speed in comparison with what the semilogarithmic relation predicts. Further, that deceleration grows roughly as u_*^2 because spray production goes roughly as u_*^3 .

I could integrate (3.11) exactly to obtain $U(z)$, but the result is an infinite series that converges very slowly. Therefore, as an alternative, I simply integrated (3.11) numerically. That integration actually computes $U(z) - U_s$, where U_s is the surface drift current, which is typically estimated as $0.5u_*$ (Wu 1975; Donelan 1998). Figure 3 shows resulting near-surface profiles of $U(z) - U_s$.

In integrating (3.11), I had to specify the boundary conditions. Even with spray present, I set $U(z_0) = U_s$, with z_0 computed from (2.13). Thus, in Fig. 3, the profiles with and without spray meet at z_0 . Since z_0 is not a physical quantity, I see no good reason why the wind speed profile with spray should have the same lower limit as the profile without spray (i.e., the semilogarithmic profile). I simply chose this lower integration

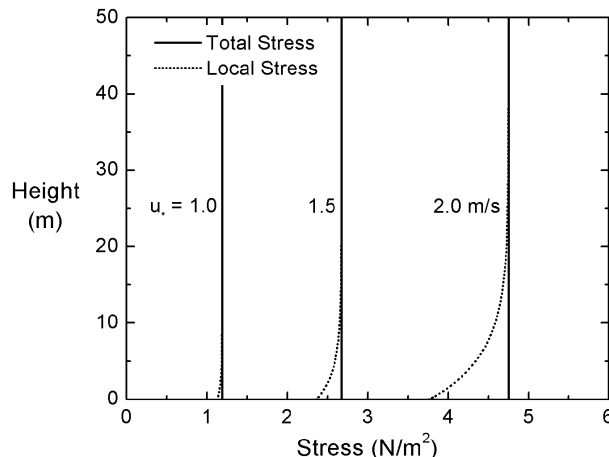


FIG. 4. Near-surface profiles of total stress τ and the local air stress, $\tau_a(z)$ in (3.1), for the same conditions as in Fig. 3.

limit because it was the most obvious arbitrary choice. Second, it provided the best physical picture: that is, with spray present, the wind speed at all levels in Fig. 3 is less than the wind speed without spray, and that difference is the most it could be.

The friction velocities depicted in Fig. 3, 1.0, 1.5, and 2.0 m s⁻¹, correspond to undisturbed 10-m winds of 21.4, 29.1, and 36.0 m s⁻¹. Thus, I have not extrapolated any of the spray parameterizations too far into unknown territory. Still, even for $u_* = 2.0$ m s⁻¹, the spray slows the 10-m wind speed by over 3 m s⁻¹. This effect is large enough to be measured if it were possible to deploy anemometers so near the surface and to retrieve data from them in such violent conditions.

The weaker near-surface velocity gradients of the profiles with spray in Fig. 3 indicate that the momentum flux in the air, $\tau_a(z)$, is less than without spray (i.e., $\tau = \rho_a u_*^2$). These gradients get weaker as the surface is approached. That is, $\tau_a(z)$ is not constant with height in the layer containing the spray; it is smallest right at the surface but increases to τ above the spray layer. Figure 4 shows these total and local air stress profiles—the latter computed from (3.2), (3.3), and (3.8)—for the same three friction velocities as in Fig. 3.

Figure 4 reiterates my assumption that the total stress is constant with height. Again, the stress that the near-surface air supports—the local stress $\tau_a(z)$ —decreases as z decreases because the spray droplets carry more and more of the stress. Figure 4 suggests that we can investigate the validity of this modeling by measuring the $\tau_a(z)$ profile near the surface with eddy-covariance techniques. If the instruments could survive in winds of 36 m s⁻¹ and could be made insensitive to the spray velocities, they would show a systematic 10% decrease between $\tau_a(z)$ values measured at 20 and at 5 m. Unfortunately, this difference is near the precision of current in situ eddy-covariance instruments. However, the fact that the stress profile in the presence of spray has the opposite behavior typically found in the atmospheric

boundary layer, where the stress generally increases toward the surface, could improve the signal-to-noise ratio.

4. Discussion

a. A sea surface transition?

My motivation for doing this study is to understand air–sea momentum exchange in high winds—of hurricane strength, 35 m s^{-1} and above. Several pieces of information suggest, however, that we cannot do as I have done and simply extrapolate what we know about air–sea transfer in winds below hurricane strength to winds above hurricane strength.

For example, Monahan and Ó Muirheartaigh's (1980) expression for the coverage W of stage-B whitecaps is

$$W = 3.84 \times 10^{-6} U_{10}^{3.41}. \quad (4.1)$$

Wu (1988) formulated an analogous expression that reads (cf. Wu 1979a)

$$W = 2 \times 10^{-6} U_{10}^{3.75}. \quad (4.2)$$

In both of these, U_{10} is the 10-m wind speed in meters per second, and W is the fractional coverage of stage-B whitecaps, which are the surface expressions of decaying bubble plumes (Monahan 1993). See also Monahan and Ó Muirheartaigh (1982), Wu (1982a, 1989), and Monahan and Woolf (1989) for discussions of these analyses.

When $U_{10} = 38.7 \text{ m s}^{-1}$, the first relation predicts $W = 1$ —the surface is totally covered in whitecaps; the second predicts $W = 1$ when $U_{10} = 33.7 \text{ m s}^{-1}$. Coincidentally, 32.7 m s^{-1} is the lower wind speed limit for Beaufort force 12, when winds are termed “hurricane” strength, and the sea is “completely white with driving spray” (Bowditch 1977).

Of course, you may argue that (4.1) and (4.2) oversimplify the whitecapping process. They do. We know, for example, that whitecap coverage also depends on the sea surface temperature because the kinematic viscosity of seawater depends strongly on water temperature (e.g., Monahan and Ó Muirheartaigh 1986; Bortkovskii 1987; Anguelova 2002). Whitecap coverage also depends on surface salinity (Monahan 1971; Anguelova 2002) and dynamic influences such as fetch, duration of the wind, and relative wind and wave orientation. As a result, (4.1) and (4.2) are accurate only to about a factor of 2.

Nevertheless, my point is that, despite their uncertainty and simplicity, (4.1) and (4.2) are compatible and suggestive. Both forecast a transition in the sea surface in the range of wind speeds between 30 and 40 m s^{-1} . I am concerned whether what we know about sea surface physics still applies beyond this transition, when the sea surface is totally bubbly and becomes “too thick to breathe and too thin to swim in” (Kraus and Businger 1994, p. 58).

A second piece of information that raises my concern about extrapolating beyond wind speeds of $30\text{--}40 \text{ m s}^{-1}$ comes from studies in wind–wave tanks and tunnels. For example, the measurements by Alamaro et al. (2002) in an annular wind–wave tank suggest that the neutral-stability, 10-m drag coefficient, $C_{\text{DN}10}$, increases roughly as we would predict from oceanic measurements (e.g., Smith 1980; Large and Pond 1981) up to 10-m wind speeds of $25\text{--}30 \text{ m s}^{-1}$ but then decreases gradually with increasing wind speed. M. A. Donelan (2003, personal communication) finds qualitatively similar behavior for $C_{\text{DN}10}$ in the Miami linear wind–wave tunnel. His $C_{\text{DN}10}$ values rise with wind speed as they do over the ocean until U_{10} reaches 33 m s^{-1} , and then they level out at this maximum value with increasing wind speed.

Alamaro et al. (2002) and M. A. Donelan (2003, personal communication) are careful, however, to explain the limitations of their laboratory observations. The tank that Alamaro et al. used was only about 1 m in diameter. Donelan's tank is 15 m long, 1 m wide, and 1 m deep, with that latter 1 m one-half air and one-half salt water. Consequently, neither tank can support the longer waves that exist at sea. Both tanks, however, do reproduce the processes that are our main interest here. That is, in high winds, the tanks exhibit continuous wave breaking, prolific spume production, whitecaps, and very bubbly water. Thus, although the scales available in laboratory tanks may mean that quantitative results obtained in them are not directly comparable to ocean results, they can help us to understand ocean processes. That is all I am arguing here: Observations in wind–wave tanks support the idea that the air–sea interface undergoes a transition in its aerodynamic behavior when the water becomes totally bubbly from intense wave breaking.

Measurements of $C_{\text{DN}10}$ over the ocean, however, are contradictory when we look for this transition. Garratt's (1977) classic review is the main reason that we believe Charnock's relation, (2.13), is valid for surface-level winds up to at least 50 m s^{-1} . He shows the drag coefficient to increase monotonically and to be well predicted by (2.13) for winds up to 50 m s^{-1} . Wu (1982b) analyzes some of the same data that Garratt used and also includes more-recent observations but reaches the same conclusion: The Charnock relation works for wind speeds up to 50 m s^{-1} . Kondo's (1975) analysis predated both of these; although he does not consider the Charnock relation, he finds the 10-m drag coefficient to increase continuously for wind speeds up to 50 m s^{-1} .

Recent observations, in contrast, suggest that $C_{\text{DN}10}$ does not increase monotonically. On the basis of the near-surface angular momentum budget in Hurricane Fredric, Kaplan, and Frank (1993) deduce the 10-m drag coefficient and conclude that it is approximately constant at 1.8×10^{-3} and displays no increase with wind speed for surface-level winds between about 20 and 40 m s^{-1} . From dropsonde profiles of the wind speed in hurricane eyewalls, Powell et al. (2003) infer that $C_{\text{DN}10}$ has behavior similar to that seen in the laboratory.

That is, they report that C_{DN10} has a maximum in the wind speed range between 30 and 40 m s^{-1} and then decreases with increasing wind speed.

The final piece of information that concerns me comes from mariners who have survived hurricane-strength winds at sea. Some have reported that the sea seemed strangely smooth (cf. Le Méhauté and Khangaonkar 1990). For example, oceanographer R. C. Beardsley (2003, personal communication) was aboard the Woods Hole ship R/V *Chain* in February 1969 in the North Atlantic near 39°N and 70°W when an extratropical storm hit. That storm was a “bomb” (Sanders and Gyakum 1980): surface-level pressure fell almost 40 hPa in 24 h, and the wind was at Beaufort force 8–12 (speeds of 19–35 m s^{-1}) for at least 1.5 days.

When Beardsley observed the sea surface during the second day of the storm, he saw it as “being quite smooth, with no small-scale waves or wave breaking.” The sea surface “was bright blue-green, like it was a mixture of water and bubbles made into foam.” He speculated “that the wind was so strong that any small-scale waves” were “instantly blown flat.” During this latter half of the storm, neither Beardsley nor the ship’s log mentions any rain that could have also explained the smoother sea surface.

Recently, instrumental observations have finally corroborated these first-hand visual observations of a smoothed sea surface, which were often deemed apocryphal. Donnelly et al. (1999) report that both C-band and Ku-band scatterometer measurements of normalized radar cross section tend to “saturate” for wind speeds above 25–30 m s^{-1} (cf. Powell et al. 2003). Because these instruments respond to radar scattering from capillary and short gravity waves, saturation implies that these waves are no longer growing with increasing wind speed. Similarly, M. A. Donelan (2003, personal communication) explains that C-band scatterometer observations of the water surface in the Miami wind-wave tunnel suggest that the “geometric roughness” of the surface decreases for effective 10-m winds above about 30 m s^{-1} .

I can envision two explanations. The bubbly sea surface might have lower surface tension and, thus, be unable to support the capillary waves that give the sea its apparent roughness. Alternatively, because of the lower tensile strength of the bubbly water (Schmelzer and Schmelzer 2003), the strong winds may simply rip the short waves right off the surface. In either case, the visually smoother sea surface might explain how the drag coefficient could level off or even decrease with increasing wind speed.

b. A “rain” of spray

In light of the spray research that I have reported here, I can think of another reason why the sea surface might appear smoother or, at least, not get rougher in high winds. To calculate the spray stress plotted in Fig.

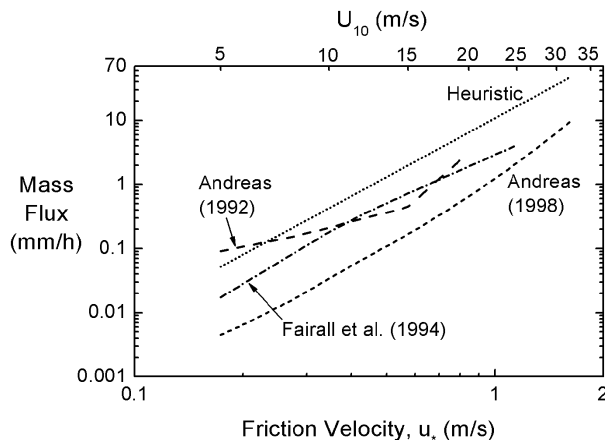


FIG. 5. The total mass flux at the sea surface associated with spray. The estimates come from inserting (2.5) in (2.2) and using the spray generation functions from Andreas (1992, 1998) and Fairall et al. (1994) for dF/dr_0 . The “Heuristic” estimate derives from (2.14).

2, I had to collect all the information necessary for computing the spray mass flux, (2.2). Figure 5 shows calculations of the total mass flux for the same three spray generation functions and for the heuristic spray stress that I used to make Fig. 2.

I plot the mass flux in Fig. 5 in units of millimeters per hour to invoke an analogy with rain at sea. The consensus is that rainfall damps waves (e.g., Tsimplis and Thorpe 1989). For instance, on the basis of a theoretical study, Le Méhauté and Khangaonkar (1990) conclude that, in one hour, a rainfall rate of 50 mm h^{-1} reduces the amplitude of meter-long waves to 62% of their original amplitude and the amplitude of 10-m waves to 95% of their original amplitude. From his theoretical study, Manton (1973) likewise concludes that a “heavy” rain of 43.2 mm h^{-1} damps out short waves (wavelengths above 1 m, say) in a few wave periods. In Manton’s model, the mechanism for this damping is the vertical mixing over the upper 10–20 cm of ocean that the raindrops produce. This mixing reduces the near-surface shear stress in the water and thereby disrupts the wave motion.

Poon et al. (1992) study rain damping in a wind-wave-rain tunnel. Each of the three rain rates they created—35, 65, and 100 mm h^{-1} —significantly damped waves with frequencies between 2 and 5 Hz (wavelengths from 40 to 6 cm). Tsimplis and Thorpe (1989) also study rain damping in a laboratory wave tank; their tank, however, had no wind. For a rainfall rate of 600 mm h^{-1} , their data show roughly a tenfold increase in the damping of waves shorter than 27 cm when compared with conditions with no rain. Although their simulated rain rate seems unnaturally heavy to me, Tsimplis and Thorpe’s results again suggest that rain preferentially damps the shortest waves.

Perhaps merely by coincidence, in Fig. 5, the heuristic model predicts that, when the wind speed reaches about 30 m s^{-1} , spray produces a “heavy” mass flux (i.e.,

greater than 30 mm h^{-1}), which proved significant for wave damping in these rain studies. That is, somewhere near a 10-m wind speed of 30 m s^{-1} , the mass flux of spray droplets falling back onto the sea surface is equivalent to a heavy rain.

The rain–wave studies that I have mentioned all agree that rain damps the shortest waves, those with wavelengths shorter than 10 m. But it is exactly these waves that support most of the interfacial surface stress (Tsimplis and Thorpe 1989; Donelan 1998; Makin and Kudryavtsev 1999). Specifically, Makin and Kudryavtsev (1999) suggest that waves shorter than 10 m support 80% of the interfacial stress, and waves shorter than 1 m support 50% of it. Since sea spray should damp waves as rain does, the obvious conclusion is that the spray could potentially make the sea surface both visually and aerodynamically smoother by quelling the short waves.

Admittedly, Manton (1973) and Le Méhauté and Khangaonkar (1990) also show that rain can generate short waves if the near-surface wind speed is much greater than the fall speed of the raindrops. Poon et al. (1992), however, seem to find no change in the rain damping in their wind–wave–rain tunnel as they increased the wind speed from 4.88 to 6.34 m s^{-1} . If the wind-driven rain were enhancing the wave growth, the effect still seemed to be smaller than the rain damping of the waves.

Another point to remember in this discussion is that rain at sea is an open system, while sea spray is a closed system. The rain falls from a relatively high-speed layer, through the slower near-surface layer, and onto the ocean, thereby carrying horizontal momentum from aloft to the surface. The spray, on the other hand, simply redistributes the near-surface momentum. Hence, I see no mechanism for falling spray to create more waves than would the wind alone in the absence of spray. I conclude that if spray has any effect on sea state, it must be to damp the shorter waves.

c. The drag coefficient with spray

Within the context of the conceptual model that I have been describing, I can make a simple estimate of how spray might affect the drag coefficient. From (3.1) and (1.1), right at the sea surface

$$\rho_a u_*^2 = \rho_a C_{D10,sp} U_{10}^2 + \tau_{sp}(0), \quad (4.3)$$

where $C_{D10,sp}$ is the 10-m drag coefficient in the presence of spray.

Inserting (2.12) and (2.14) in (4.3) and rearranging terms, I get

$$C_{D10,sp} = \left[1 - 6.5 \times 10^{-5} \left(\frac{\rho_w}{\rho_a} \right) u_*^2 \right] \left[\frac{k}{\ln(10/z_0)} \right]^2. \quad (4.4)$$

To calculate $C_{D10,sp}$ from (4.4), I use (2.13) to specify z_0 .

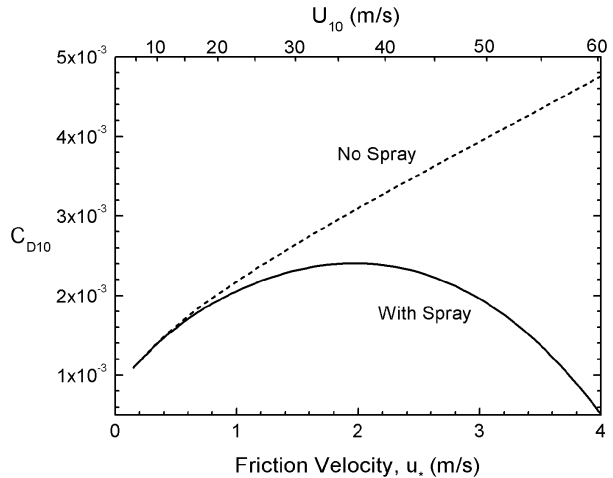


FIG. 6. Estimates of the 10-m, neutral-stability drag coefficient with (i.e., $C_{D10,sp}$) and without (i.e., C_{DN10}) spray present. The “With Spray” result comes from (4.4); the “No Spray” result comes from (4.5) and (2.13) and essentially parameterizes the total stress τ . For these calculations, the air temperature is 26°C , and the barometric pressure is 1000 hPa .

Figure 6 shows C_{DN10} and $C_{D10,sp}$. The C_{DN10} here is the neutral-stability, 10-m drag coefficient associated with the total stress, τ in (3.1) [or $\rho_a u_*^2$ in (4.3)], and is just

$$C_{DN10} = \left[\frac{k}{\ln(10/z_0)} \right]^2 \quad (4.5)$$

by definition. It increases monotonically with u_* because the roughness length in (4.5), modeled with Charnock’s relation (2.13), increases with u_* . However, because the spray supports an increasing amount of the momentum flux as u_* increases, (4.4) suggests that $C_{D10,sp}$ reaches a maximum but then starts decreasing. Coincidentally, this maximum corresponds to a 10-m wind speed between 30 and 40 m s^{-1} .

Realize that I present (4.4) and Fig. 6 as suggestive rather than conclusive. To derive (4.4), I assume that (2.12) describes the 10-m wind, but Fig. 3 already shows that (2.12) overestimates U_{10} when spray is present. The effect of this assumption is that (4.4) will underestimate $C_{D10,sp}$ by, perhaps, 20%–30% for the highest u_* values in Fig. 6.

On the other hand, in deriving (4.4), I ignored the wave damping of the spray. In effect, this damping would reduce z_0 from what (2.13) predicts and, therefore, would make $C_{D10,sp}$ smaller. That is, by ignoring spray damping, (4.4) predicts $C_{D10,sp}$ to be larger than it should be.

In light of these offsetting effects, Fig. 6 seems qualitatively reasonable (though probably not quantitatively). I could, of course, easily include the effects of the spray on U_{10} in (4.3) and subsequently in Fig. 6, but the simple result (4.4), without that effect, is fairly transparent. The complexity that this detail would have added

to the calculations also seemed unwarranted since I do not have enough information to estimate the magnitude of the offsetting effect of the spray wave damping.

Let me reiterate that (4.3) applies right at the sea surface. That is, by definition $\rho_a C_{D10,sp} U_{10}^2 = \tau_a(0)$. Realize, too, that the values of the drag coefficient that Powell et al. (2003) report *do not* corroborate Fig. 6 or vice versa: We are analyzing different drag coefficients. My $C_{D10,sp}$ models the surface stress that the frictional drag of the air supports, $\tau_a(0)$ in (3.1). On the other hand, the drag coefficient that Powell et al. deduce relates the total surface stress τ to U_{10} and is really an estimate of C_{DN10} in (4.5).

Experimentally confirming the prediction in Fig. 6 may be difficult. The standard way to measure τ_a is with eddy-correlation instruments placed several meters above the surface (e.g., Kaimal and Finnigan 1994, p. 219) and then to assume that this measurement is equal to the surface stress, $\tau_a(0)$. However, as I have shown, when spray is present, τ_a is not constant with height. We would need to extrapolate the measured stress to the surface to obtain an experimental value of $C_{D10,sp}$. Equation (3.1) and Fig. 4 could be a basis for this extrapolation.

5. Conclusions

Conceptually, spray's ability to alter the distribution of momentum in the near-surface droplet layer is easy to understand. Once created, spray droplets accelerate almost immediately to the local wind speed (see Fig. 1). This process extracts momentum from the wind and therefore slows the wind near the surface (see Fig. 3). However, these droplets are massive and eventually fall back into the sea, carrying the horizontal momentum that they have extracted from the wind with them.

Based on several reliable estimates of the spray generation function—the rate at which spray droplets of initial radius r_0 are created as a function of wind speed—I estimated the rate at which the spray extracts momentum from the wind and, in turn, delivers it to the sea. This spray stress increases roughly as the fourth power of the friction velocity u_* and, thus, will eventually become comparable to the total stress, which increases only as the square of u_* (see Fig. 2). I estimate that the spray supports all of the surface stress when the wind speed reaches about 60 m s^{-1} , and the spray stress carries 10% of the total stress when the wind speed is about 30 m s^{-1} .

Besides redistributing momentum, sea spray likely has an effect on sea state in very high winds. Rain has been shown to damp short waves (those with wavelengths less than 10 m). My calculations suggest that the mass flux of spray falling back on the ocean is comparable to a “heavy” rain when the wind speed reaches about 30 m s^{-1} . Spray must therefore also damp short waves in high winds. The effect would be to make

the sea surface appear visually and aerodynamically smoother.

The implication here is that sea spray plays a key role in a negative feedback loop that limits air–sea momentum exchange, as required by some hurricane models (e.g., Emanuel 1995; Andreas and Emanuel 2001). Wind builds waves. When the wind is strong enough and the waves get high enough, they produce copious spray. The spray droplets, however, eventually plunge back to the sea and flatten the shortest waves, which extract much of the momentum from the wind that is turned to wave growth. If all of the steps in this loop ultimately reach comparable magnitudes, the energy in the wave spectrum, at least at the shortest wavelengths, must be limited. In turn, the air-to-sea momentum flux must be limited.

Those spray results and the estimates of whitecap coverage that I reviewed in the last section suggest that the sea surface experiences a transition in the wind speed range $30\text{--}40 \text{ m s}^{-1}$, when several processes combine to make it aerodynamically smoother. Very simple mathematics, represented in (4.4) and in Fig. 6, bring this point to light. My results suggest that the 10-m drag coefficient that models the frictional drag of the air on the sea surface reaches a peak of about 2.4×10^{-3} in the wind speed range $30\text{--}40 \text{ m s}^{-1}$ and then decreases to about one-half of the value it has in light winds by the time the wind speed reaches 60 m s^{-1} .

My work has basically ignored how the spectrum of wind waves changes with wind speed. The shape of this spectrum is admittedly crucial to understanding how the surface stress is partitioned between skin friction and form drag in low and moderate winds. However, as the sea undergoes the transition to a totally bubbly surface in the wind speed range $30\text{--}40 \text{ m s}^{-1}$, spray processes assume increasing importance. We could reasonably speculate that spray processes dominate the air–sea exchange mechanism in wind speeds above 50 m s^{-1} (cf. Emanuel 2003).

Acknowledgments. I thank Kerry A. Emanuel for several discussions that helped to clarify my thinking on this subject, Edward C. Monahan for insightful comments on the manuscript, Robert C. Beardsley for the account of his storm encounter and copies of the *Chain's* log of the event, and two anonymous reviewers for helping me to smooth out the rough sections. The Office of Naval Research supported this work with Award N0001403MP20010; the National Science Foundation supported it with Award ATM-00-01037.

REFERENCES

- Alamaro, M., K. Emanuel, J. Colton, W. McGillis, and J. Edson, 2002: Experimental investigation of air–sea transfer of momentum and enthalpy at high wind speeds. Preprints, *25th Conf. on Hurricanes and Tropical Meteorology*, San Diego, CA, Amer. Meteor. Soc., 667–668.

- Andreas, E. L., 1990: Time constants for the evolution of sea spray droplets. *Tellus*, **42B**, 481–497.
- , 1992: Sea spray and the turbulent air–sea heat fluxes. *J. Geophys. Res.*, **97**, 11 429–11 441.
- , 1998: A new sea spray generation function for wind speeds up to 32 m s^{-1} . *J. Phys. Oceanogr.*, **28**, 2175–2184.
- , 2002: A review of the sea spray generation function for the open ocean. *Atmosphere–Ocean Interactions*, Vol. 1, W. Perrie, Ed., WIT Press, 1–46.
- , and J. DeCosmo, 1999: Sea spray production and influence on air–sea heat and moisture fluxes over the open ocean. *Air–Sea Exchange: Physics, Chemistry and Dynamics*, G. L. Geernaert, Ed., Kluwer, 327–362.
- , and K. A. Emanuel, 2001: Effects of sea spray on tropical cyclone intensity. *J. Atmos. Sci.*, **58**, 3741–3751.
- , J. B. Edson, E. C. Monahan, M. P. Rouault, and S. D. Smith, 1995: The spray contribution to net evaporation from the sea: A review of recent progress. *Bound.-Layer Meteor.*, **72**, 3–52.
- Angelova, M. D., 2002: Whitecaps, sea-salt aerosols, and climate. Ph.D. dissertation, University of Delaware, 248 pp.
- Belcher, S. E., and J. C. R. Hunt, 1993: Turbulent shear flow over slowly moving waves. *J. Fluid Mech.*, **251**, 109–148.
- Bintanja, R., 1998: The interaction between drifting snow and atmospheric turbulence. *Ann. Glaciol.*, **26**, 167–173.
- Bortkovskii, R. S., 1987: *Air–Sea Exchange of Heat and Moisture During Storms*. D. Reidel, 194 pp.
- Bowditch, N., 1977: *American Practical Navigator*, Vol. 1, Publ. 9, Defense Mapping Agency Hydrographic Center, 1386 pp.
- Caldwell, D. R., and W. P. Elliott, 1971: Surface stresses produced by rainfall. *J. Phys. Oceanogr.*, **1**, 145–148.
- , and —, 1972: The effect of rainfall on the wind in the surface layer. *Bound.-Layer Meteor.*, **3**, 146–151.
- Clift, R., J. R. Grace, and M. E. Weber, 1978: *Bubbles, Drops, and Particles*. Academic Press, 380 pp.
- de Leeuw, G., 1986: Vertical profiles of giant particles close above the sea surface. *Tellus*, **38B**, 51–61.
- , 1987: Near-surface particle size distribution profiles over the North Sea. *J. Geophys. Res.*, **92**, 14 631–14 635.
- Donelan, M. A., 1998: Air–water exchange processes. *Physical Processes in Lakes and Oceans*, J. Imberger, Ed., Coastal and Estuarine Studies, Vol. 54, Amer. Geophys. Union, 19–36.
- Donnelly, W. J., J. R. Carswell, R. E. McIntosh, P. S. Chang, J. Wilkerson, F. Marks, and P. G. Black, 1999: Revised ocean backscatter models at C and Ku band under high-wind conditions. *J. Geophys. Res.*, **104**, 11 485–11 497.
- Edson, J. B., S. Anquetin, P. G. Mestayer, and J. F. Sini, 1996: Spray droplet modeling: 2. An interactive Eulerian–Lagrangian model of evaporating spray droplets. *J. Geophys. Res.*, **101**, 1279–1293.
- Emanuel, K. A., 1995: Sensitivity of tropical cyclones to surface exchange coefficients and a revised steady-state model incorporating eye dynamics. *J. Atmos. Sci.*, **52**, 3969–3976.
- , 1999: Thermodynamic control of hurricane intensity. *Nature*, **401**, 665–669.
- , 2003: A similarity hypothesis for air–sea exchange at extreme wind speeds. *J. Atmos. Sci.*, **60**, 1420–1428.
- Fairall, C. W., and S. E. Larsen, 1984: Dry deposition, surface production and dynamics of aerosols in the marine boundary layer. *Atmos. Environ.*, **18**, 69–77.
- , J. B. Edson, and M. A. Miller, 1990: Heat fluxes, whitecaps, and sea spray. *Surface Waves and Fluxes*, Vol. 1, G. L. Geernaert and W. J. Plant, Eds., Kluwer, 173–208.
- , J. D. Kepert, and G. J. Holland, 1994: The effect of sea spray on surface energy transports over the ocean. *Global Atmos. Ocean Syst.*, **2**, 121–142.
- Garratt, J. R., 1977: Review of drag coefficients over oceans and continents. *Mon. Wea. Rev.*, **105**, 915–929.
- Hara, T., and S. E. Belcher, 2002: Wind forcing in the equilibrium range of wind-wave spectra. *J. Fluid Mech.*, **470**, 223–245.
- Johnson, H. K., J. Højstrup, H. J. Vested, and S. E. Larsen, 1998: On the dependence of sea surface roughness on wind waves. *J. Phys. Oceanogr.*, **28**, 1702–1716.
- Kaimal, J. C., and J. J. Finnigan, 1994: *Atmospheric Boundary Layer Flows: Their Structure and Measurement*. Oxford University Press, 289 pp.
- Kaplan, J., and W. M. Frank, 1993: The large-scale inflow-layer structure of Hurricane Fredric. *Mon. Wea. Rev.*, **121**, 3–20.
- Kondo, J., 1975: Air–sea bulk transfer coefficients in diabatic conditions. *Bound.-Layer Meteor.*, **9**, 91–112.
- Kraus, E. B., and J. A. Businger, 1994: *Atmosphere–Ocean Interaction*. 2d ed. Oxford University Press, 362 pp.
- Kudryavtsev, V. N., and V. K. Makin, 2001: The impact of air-flow separation on the drag of the sea surface. *Bound.-Layer Meteor.*, **98**, 155–171.
- Large, W. G., and S. Pond, 1981: Open ocean momentum flux measurements in moderate to strong winds. *J. Phys. Oceanogr.*, **11**, 324–336.
- Le Méhauté, B., and T. Khangaonkar, 1990: Dynamic interaction of intense rain with water waves. *J. Phys. Oceanogr.*, **20**, 1805–1812.
- Lighthill, J., 1999: Ocean spray and the thermodynamics of tropical cyclones. *J. Eng. Math.*, **35**, 11–42.
- Makin, V. K., and V. N. Kudryavtsev, 1999: Coupled sea surface-atmosphere model. 1. Wind over waves coupling. *J. Geophys. Res.*, **104**, 7613–7623.
- Manton, M. J., 1973: On the attenuation of sea waves by rain. *Geophys. Fluid Dyn.*, **5**, 249–260.
- Mestayer, P. G., A. M. J. van Eijk, G. de Leeuw, and B. Tranchant, 1996: Numerical simulation of the dynamics of sea spray over the waves. *J. Geophys. Res.*, **101**, 20 771–20 797.
- Monahan, E. C., 1966: Sea spray and its relationship to low elevation wind speed. Ph.D. dissertation, Massachusetts Institute of Technology, 147 pp.
- , 1971: Oceanic whitecaps. *J. Phys. Oceanogr.*, **1**, 139–144.
- , 1993: Occurrence and evolution of acoustically relevant subsurface bubble plumes and their associated, remotely monitorable, surface whitecaps. *Natural Physical Sources of Underwater Sound*, B. R. Kerman, Ed., Kluwer, 503–517.
- , and I. G. Ó Muircheartaigh, 1980: Optimal power-law description of oceanic whitecap coverage dependence on wind speed. *J. Phys. Oceanogr.*, **10**, 2094–2099.
- , and —, 1982: Reply. *J. Phys. Oceanogr.*, **12**, 751–752.
- , and —, 1986: Whitecaps and the passive remote sensing of the ocean surface. *Int. J. Remote Sens.*, **7**, 627–642.
- , and D. K. Woolf, 1989: Comments on “Variations of whitecap coverage with wind stress and water temperature.” *J. Phys. Oceanogr.*, **19**, 706–709.
- Moore, D. J., and B. J. Mason, 1954: The concentration, size distribution and production rate of large salt nuclei over the oceans. *Quart. J. Roy. Meteor. Soc.*, **80**, 583–590.
- Munk, W. H., 1955: Wind stress over water: An hypothesis. *Quart. J. Roy. Meteor. Soc.*, **81**, 320–332.
- Pielke, R. A., and T. J. Lee, 1991: Influence of sea spray and rainfall on the surface wind profile during conditions of strong winds. *Bound.-Layer Meteor.*, **55**, 305–308.
- Pomeroy, J. W., and D. H. Male, 1987: Wind transport of seasonal snowcovers. *Seasonal Snowcovers: Physics, Chemistry, Hydrology*, H. G. Jones and W. J. Orville-Thomas, Eds., D. Reidel, 119–140.
- Poon, Y.-K., S. Tang, and J. Wu, 1992: Interactions between rain and wind waves. *J. Phys. Oceanogr.*, **22**, 976–987.
- Powell, M. D., P. J. Vickery, and T. A. Reinhold, 2003: Reduced drag coefficient for high wind speeds in tropical cyclones. *Nature*, **422**, 279–283.
- Press, W. H., S. A. Teukolsky, W. T. Vetterling, and B. P. Flannery, 1992: *Numerical Recipes in FORTRAN: The Art of Scientific Computing*. 2d ed. Cambridge University Press, 963 pp.
- Radok, U., 1968: Deposition and erosion of snow by the wind. Res. Rep. 230, U.S. Army Cold Regions Research and Engineering Laboratory, Hanover, NH, 23 pp.

- Raupach, M. R., 1991: Saltation layers, vegetation canopies and roughness lengths. *Acta Mech.*, **1** (Suppl.), 83–96.
- Rouault, M. P., P. G. Mestayer, and R. Schiestel, 1991: A model of evaporating spray droplet dispersion. *J. Geophys. Res.*, **96**, 7181–7200.
- Sanders, F., and J. R. Gyakum, 1980: Synoptic-dynamic climatology of the “Bomb.” *Mon. Wea. Rev.*, **108**, 1589–1606.
- Schmelzer, J. W. P., and J. Schmelzer Jr., 2003: Kinematics of bubble formation and the tensile strength of liquids. *Atmos. Res.*, **65**, 303–324.
- Schmidt, R. A., 1982: Vertical profiles of wind speed, snow concentration, and humidity in blowing snow. *Bound.-Layer Meteor.*, **23**, 223–246.
- Smith, S. D., 1980: Wind stress and heat flux over the ocean in gale force winds. *J. Phys. Oceanogr.*, **10**, 709–726.
- Toba, Y., 1965: On the giant sea-salt particles in the atmosphere: II. Theory of the vertical distribution in the 10-m layer over the ocean. *Tellus*, **17**, 365–382.
- , S. D. Smith, and N. Ebuchi, 2001: Historical drag expressions. *Wind Stress over the Ocean*, I. S. F. Jones and Y. Toba, Eds., Cambridge University Press, 35–53.
- Tsimplis, M., and S. A. Thorpe, 1989: Wave damping by rain. *Nature*, **342**, 893–895.
- Wamser, C., and V. N. Lykossov, 1995: On the friction velocity during blowing snow. *Beitr. Phys. Atmos.*, **68**, 85–94.
- Wu, J., 1973: Spray in the atmospheric surface layer: Laboratory study. *J. Geophys. Res.*, **78**, 511–519.
- , 1975: Wind-induced drift currents. *J. Fluid Mech.*, **68**, 49–70.
- , 1979a: Oceanic whitecaps and sea state. *J. Phys. Oceanogr.*, **9**, 1064–1068.
- , 1979b: Spray in the atmospheric surface layer: Review and analysis of laboratory and oceanic results. *J. Geophys. Res.*, **84**, 1693–1704.
- , 1982a: Comments on “Optimal power-law description of oceanic whitecap coverage dependence on wind speed.” *J. Phys. Oceanogr.*, **12**, 750–751.
- , 1982b: Wind-stress coefficients over sea surface from breeze to hurricane. *J. Geophys. Res.*, **87**, 9704–9706.
- , 1988: Variations of whitecap coverage with wind stress and water temperature. *J. Phys. Oceanogr.*, **18**, 1448–1453.
- , 1989: Reply. *J. Phys. Oceanogr.*, **19**, 710–711.
- Xiao, J., and P. A. Taylor, 2002: On equilibrium profiles of suspended particles. *Bound.-Layer Meteor.*, **105**, 471–482.